CHIN. PHYS. LETT. Vol. 34, No. 10 (2017) 107101

First-Principles Calculation for the Half Metallic Properties of La_2NbMnO_6 *

Ning-Ning Zu(祖宁宁)**, Rui Li(李瑞), Ya-Hui Zheng(郑亚辉), Lin Chen(陈林)

Department of Physics, College of Science, Qiqihar University, Qiqihar 161006

(Received 11 April 2017)

La_2VMnO_6 is measured to be insulating and ferrimagnetic experimentally. In this study, by substituting V with Nb, La_2NbMnO_6 is investigated using the density functional theory. The calculated results indicate that La_2NbMnO_6 is also ferrimagnetic and exhibits the half metallic properties due to the strong electron correlation of Mn. The valence states of Nb and Mn are assigned to be +4 and +2 in La_2NbMnO_6, respectively, which are different from V^{3+}/Mn^{3+} in La_2VMnO_6.

PACS: 71.15.Mb, 71.20.−b, 71.20.Be, 72.25.Ba DOI: 10.1088/0256-307X/34/10/107101

Half metallic (HM) materials are a class of materials which are metallic in one spin direction while semiconducting or insulating in the opposite spin channel.[1] They have 100% spin polarization at the Fermi level, and are expected to play a vital role in the spintronic devices using the spin-polarized conduction carriers. Double-perovskite oxide $A_2BB'O_6$ has attracted intense research activities in searching HM compounds[2−9] due to variation of the magnetic (or non-magnetic) B and B' elements as well as the A-site cations. Among them, Pickett[3] designed the compound La_2VMnO_6, and assumed that it has a cubic structure and Mn^{3+} is in a low spin state. The band structure calculation results demonstrate that La_2VMnO_6 is a compensated half metal, i.e., half metal with zero net magnetic moment. Later, the partially ordered single-phase[10] La_2VMnO_6 and B-site ordered La_2VMnO_6 thin film[11,12] were synthesized experimentally, both of them have a cubic structure ($Fm\bar{3}m$ space group). However, the measurement results show that, contrary to the earlier theoretical prediction,[3] the electronic ground state of this material is insulating, and the system exhibits a ferrimagnetic (FiM) state rather than an antiferromagnetic (AFM) one owing to Mn^{3+} taking a high spin state instead of a low spin state. To explain the discrepancy between theoretical and experimental studies, the compound was revisited using the density functional theory.[13] It is found that the experimentally observed insulating FiM properties can be reproduced by the cooperative effect of electron correlation and spin–orbit coupling (SOC).

With respect to the 3d transition elements, the 4d ones have wider band and smaller electron correlation, as well as more pronounced SOC effect. Therefore, if a 3d element in perovskite is substituted with a 4d element, the transport property of the material may occur significantly. Motivated by this idea, in this work, we substitute the 3d V with the same column element 4d Nb in La_2VMnO_6, i.e., La_2NbMnO_6. We investigate the electron and magnetic properties of La_2NbMnO_6 and discuss the influences of electron correlation and SOC, expecting to obtain a new material with HM properties.

Geometry optimizations were performed by employing Vienna *ab initio* simulation package (VASP),[14−17] based on the projector augmented wave (PAW) method.[18,19] For the self-consistent calculation, the plane wave cutoff energy was chosen to be 500 eV. A mesh of $5 \times 5 \times 5$ k-points was used. The convergence tolerances were selected as the difference in total energy and the maximum force within 1.0×10^{-5} eV and 1.0×10^{-2} eV/Å, respectively.

The electronic and magnetic properties were calculated using the WIEN2K program,[20,21] which is based on the full-potential linearized augmented plane wave (FPLAPW) method. The atomic sphere radii $R_{\rm MT}$ were 2.40, 1.90, 2.00 and 1.60 bohrs for La, Nb, Mn and O, respectively. In the complete Brillouin zone, 1000 k-points were used. The plane wave expansion cutoff is $R_{\rm MT}^{\rm min}K_{\rm max} = 7.0$ for expanding the wave function, where $R_{\rm MT}^{\rm min}$ is the atomic sphere radius, and $K_{\rm max}$ is the plane wave cutoff. The self-consistent calculations were considered to be converged when the energy convergence was less than 10^{-5} Ry/f.u. (f.u. indicates formula unit). The exchange-correlation energy was treated by the generalized gradient approximation (GGA-PBE).[22] Electron correlation for the transition elements in combination with the double-counting correlation was considered in the rotationally invariant form with a single effective Hubbard parameter $U_{\rm eff} = U - J$,[23] where U and J stand for the Coulomb and exchange parameters, respectively. For simplicity, we use U instead of $U_{\rm eff}$ in the following.

*Supported by the Scientific Research Plan Projects of Heilongjiang Education Department under Grant No 135109311, the National Natural Science Foundation of China under Grant Nos 11404180 and 11405092, and the Natural Science Foundation of Heilongjiang Province under Grant Nos A2015010 and B201420.

**Corresponding author. Email: nn.zu@163.com

© 2017 Chinese Physical Society and IOP Publishing Ltd

A series of U values are selected for transition metals, i.e., 1.5, 2.5, 3.5 eV for Nb, and 3.0, 4.0, 5.0 eV for Mn, while $J = 0.0$. These values have been adopted in La_2VMnO_6.[13] Since the main conclusions are not sensitive to the choice of selected U values, we choose the results from $U_{Nb} = 3.5$ eV, $U_{Mn} = 5.0$ eV for further discussion. Considering the large effect of SOC on transition metal atoms, especially $4d$ and $5d$ ones, we also include calculating the electronic and magnetic properties based on the second-variational method using the scalar relativistic wave functions.[24]

The same crystal structure as La_2VMnO_6, cubic $Fm\bar{3}m$, is adopted for La_2NbMnO_6, as shown in Fig. 1. The optimized lattice parameter is 8.069 Å, larger than the experimental value 7.838 Å of La_2VMnO_6.[11] The enlargement of the cell volume after substituting partially arises from the computational methods that would overestimate the lattice constants. The other reason is associated to variation of the ionic radii of the transition metals, which will be discussed in the following. The atom coordinates for La_2NbMnO_6 are listed in Table 1. In addition, the obtained Nb–O bond length is 2.023 Å, and Mn–O is 2.012 Å.

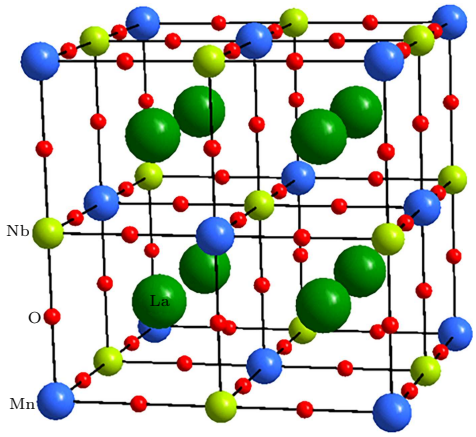

Fig. 1. Crystal structure of La_2NbMnO_6.

Table 1. Wyckoff sites and fractional coordinates for La_2NbMnO_6.

	Atom	Site	Coordinates
La_2NbMnO_6	La	8c	(1/4, 1/4, 1/4)
	Mn	4a	(0, 0, 0)
$Fm\bar{3}m$ (No. 225)	Nb	4b	(1/2, 1/2, 1/2)
	O	24e	(0.2507, 0, 0)

Here we consider four magnetic configurations to determine the magnetic ground state of La_2NbMnO_6, ferromagnetic (FM), FiM, A-type AFM (AFM interplanar and FM intraplanar coupling) and C-type AFM (AFM coupling for the adjacent chains along c-direction) states. The result indicates that the FiM state is the most energy favorable. In other words, the antiparallel arrangement between the two magnetic ions is retained after substituting V with Nb in La_2VMnO_6.

To dissect the important roles of electron correlation and SOC on the nature of La_2NbMnO_6, Fig. 2 presents the calculated orbital-decomposed density of states (DOS) using four methods. For GGA approach (Fig. 2(a)), in the spin-up direction, the conducting electrons are mainly contributed by the partially filled Nb t_{2g} manifold, and in the opposite spin channel, the Fermi level just stands at the top of the Mn e_g band. Hence, La_2NbMnO_6 can be considered to be at the end point of normal metal-half metal transition for GGA. After including the electron correlation (GGA+U, Fig. 2(b)), unexpectedly it is found that the DOS of Nb $4d$ almost remains the original (even though the value of U_{Nb} is set up to 6.0 eV, the case is still). This indicates that the electron correlation has no effect on Nb in our system. In contrast, the Mn $3d$ (t_{2g} and e_g) spin-up and spin-down orbitals are pulled further to the higher and lower energy region after pulsing U, respectively. The exchange splitting increases from ∼4.0 eV to ∼7.5 eV accordingly. Therefore, La_2NbMnO_6 turns out to be a half metal. The spin magnetic moment of Mn increases from 3.51μ_B to 4.28μ_B (Table 2) due to more localization of d state. As for the somewhat decreased spin magnetic moment of Nb (from 0.30μ_B to 0.21μ_B, Table 2), it may be induced by the weaker hybridization near the region of the Fermi level between the Nb and Mn t_{2g} spin-up bands after regarding the electron correlation. On the other hand, when considering the SOC, further energy splitting will occur. In our cubic structure, t_{2g} are split into singlet d_{xy} level and doubly degenerate $d_{xz}+d_{yz}$ level, and e_g into singlet d_{x2-y2} and d_{z2} levels (GGA+SOC, Fig. 2(c)). These nondegenerate bands, however, overlap with each other, thus the DOS profile has little change compared to that in GGA.

Given their respective roles of the electron correlation and SOC, Fig. 2(d) shows the results by considering the GGA+U and GGA+U+SOC simultaneously. It can be seen that the split levels caused by SOC still overlap with each other, and the function of U is only to increase the exchange splitting of Mn $3d$ orbitals as before. This means that the electron correlation and SOC work separately in GGA+U+SOC, and there is no interaction between them[25–27] in our system. Naturally, the new property of the compound resulted from this kind of interaction is not observed. Here we can obtain that the HM nature of La_2NbMnO_6 is attributed to the electron correlation of Mn rather than the SOC effect. The case in La_2NbMnO_6 is quite different from that in La_2VMnO_6, where the experimentally observed insulating nature of La_2VMnO_6 is reproduced by the cooperative effect of U and SOC.[13] Moreover, the orbital moments of Nd and Mn are both tiny (0.04μ_B and 0.00μ_B, Table 2), which illustrates the quite weak effect of SOC in La_2NbMnO_6.

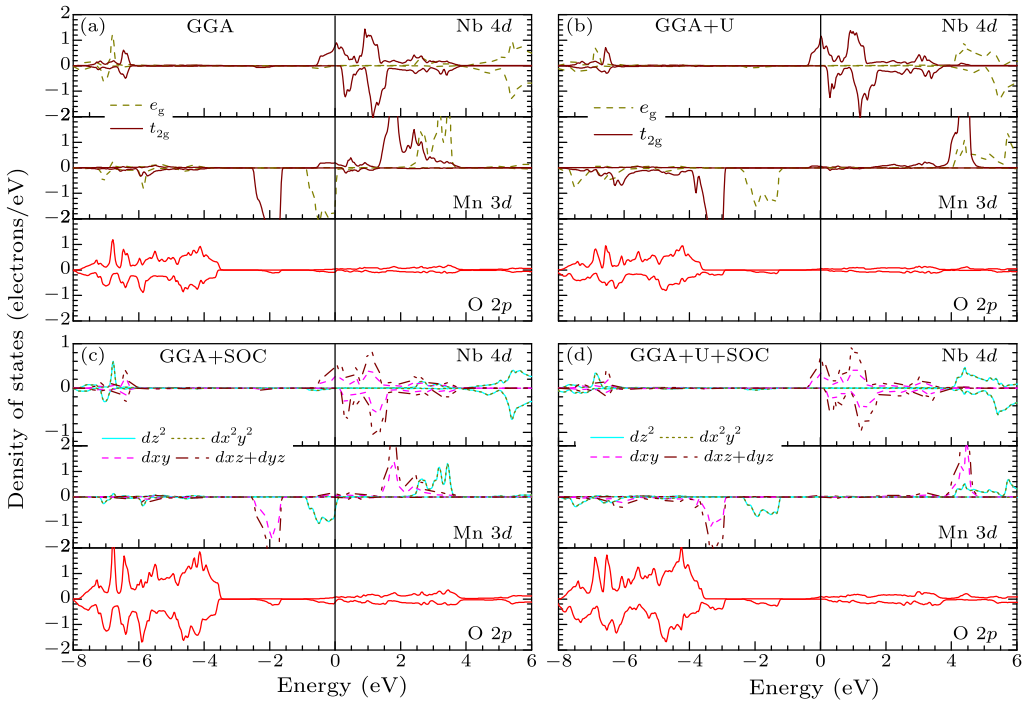

Fig. 2. Calculated orbital-decomposed density of states for La_2NbMnO_6 from (a) GGA, (b) GGA+U, (c) GGA+SOC and (d) GGA+U+SOC methods. The vertical lines indicate the Fermi energy level. Here $U_{Nb} = 3.5$ eV and $U_{Mn} = 5.0$ eV.

Table 2. Individual and net magnetic moments (μ_B) of La_2NbMnO_6. The net magnetic moment is the sum of total spin and total orbital moments. Here $U_{Nb} = 3.5$ eV, $U_{Mn} = 5.0$ eV.

	$M^{spin}_{Nb/V}$	M^{spin}_{Mn}	M^{spin}_{Total}	$M^{orb}_{Nb/V}$	M^{orb}_{Mn}	M^{orb}_{Total}	M^{net}_{Total}
GGA	0.30	−3.51	−3.02				
GGA+U	0.21	−4.28	−4.05				
GGA+SOC	0.30	−3.51	−3.04	−0.03	0.00	−0.03	−3.07
GGA+U+SOC	0.21	−4.28	−4.05	−0.04	0.00	−0.04	−4.09

In the light of the DOS property of the full occupation of the Mn 3d spin-down orbital in GGA+U (and GGA+U+SOC), the valence state of Mn in La_2NbMnO_6 can be assigned to be +2 in the ionic model, and then Nb to be +4. The determined valence states can also be supported by the spin moments of Nb and Mn (Table 2) although these moments are somewhat reduced due to the p–d hybridization. Note that both V and Mn are +3 in La_2VMnO_6.[13] Thus the valence states of both the magnetic ions in the compound have changed after substituting V with Nb. From V^{3+}/Mn^{3+} to Nb^{4+}/Mn^{2+}, the charge difference between the two transition metal ions at B sites becomes larger, which will reduce the possibility of anti-site defects and will be beneficial for the structure order. In addition, the radius of Nb^{4+} (0.68 Å) is larger than that of V^{3+} (0.64 Å), and the radius of Mn^{2+} (0.83 Å) is also larger than that of Mn^{3+} (0.645 Å). This is another reason for the enlargement of the cell volume of La_2NbMnO_6 compared with La_2VMnO_6.

In summary, we have designed the compound of La_2NbMnO_6 based on the insulating ferrimagnet La_2VMnO_6, and performed the first-principle calculations to investigate its electronic and magnetic properties. Our calculated results indicate that the FiM state is still the magnetic ground state after substituting V with Nb. Electron correlation and SOC are considered during the calculation. However, the electron correlation almost has no influence on Nb, and the effects of SOC on both Nb and Mn are quite weak. Meanwhile, there is no synergistic action between the electron correlation and SOC in our system. Consequently, La_2NbMnO_6 demonstrates the properties of half metal, and this nature is attributed to the strong electron correlation of Mn. In contrast to V^{3+}/Mn^{3+} in La_2VMnO_6, the valence states of Nb and Mn are assigned to be +4 and +2 in La_2NbMnO_6, respectively.

References

[1] de Groot R A, Mueller F M, van Engen P G and Buschow K H J 1983 *Phys. Rev. Lett.* **50** 2024
[2] Lee W K and Pickett W E 2008 *Phys. Rev.* B **77** 115101
[3] Pickett W E 1998 *Phys. Rev.* B **57** 10613
[4] Park J H, Kwon S K and Min B I 2002 *Phys. Rev.* B **65** 174401

[5] Park M S and Min B I 2005 *Phys. Rev.* B **71** 052405
[6] Wang Y K and Guo G Y 2006 *Phys. Rev.* B **73** 064424
[7] Pardo V and Pickett W E 2009 *Phys. Rev.* B **80** 054415
[8] Chen S H, Xiao Z R, Liu Y P and Wang Y K 2010 *J. Appl. Phys.* **108** 093908
[9] Sanyal P, Halder A, Si L, Wallerberger M, Held K and Saha-Dasgupta T 2016 *Phys. Rev.* B **94** 035132
[10] Androulakis J, Katsarakis N and Giapintzakis J 2002 *Solid State Commun.* **124** 77
[11] Chakraverty S, Yoshimatsu K, Kozuka Y, Kumigashira H, Oshima M, Makino T, Ohtomo A and Kawasaki M 2011 *Phys. Rev.* B **84** 132411
[12] Ohtomo A, Chakraverty S, Mashiko H, Oshima T and Kawasaki M 2013 *J. Mater. Res.* **28** 689
[13] Zu N N, Wang J and Wu Z J 2013 *J. Phys. Chem.* C **117** 7231
[14] Kresse G and Hafner J 1993 *Phys. Rev.* B **47** 558
[15] Kresse G and Hafner J 1994 *Phys. Rev.* B **49** 14251
[16] Kresse G and Furthmüller J 1996 *Comput. Mater. Sci.* **6** 15
[17] Kresse G and Furthmüller J 1996 *Phys. Rev.* B **54** 11169
[18] Blöchl P E 1994 *Phys. Rev.* B **50** 17953
[19] Kresse G and Joubert D 1999 *Phys. Rev.* B **59** 1758
[20] Schwarz K and Blaha P 2003 *Comput. Mater. Sci.* **28** 259
[21] Blaha P, Schwarz K, Madsen G K H, Kvasnicka D, Luitz J 2001 *WIEN2K: An Augmented Plane Wave and Local Orbitals Program for Calculating Crystal Properties* (Vienna: Technical University Wien)
[22] Perdew J P, Burke K and Ernzerhof M 1996 *Phys. Rev. Lett.* **77** 3865
[23] Liechtenstein A I, Anisimov V I and Zaanen J 1995 *Phys. Rev.* B **52** R5467
[24] Kunes J, Novak P, Divis M and Oppeneer P M 2001 *Phys. Rev.* B **63** 205111
[25] Lv S H, Liu X J, Li H P, Han L, Wang Z C and Meng J 2012 *J. Comput. Chem.* **33** 1433
[26] Wang J P, Song W Y and Wu Z J 2010 *Phys. Status Solidi* B **247** 194
[27] Jin S H and Lee W K 2011 *Phys. Rev.* B **84** 172405